Preprints of the 5th IFAC Symposium on Mechatronic Systems
Marriott Boston Cambridge
Cambridge, MA, USA, September 13-15, 2010

Multiobjective Time Domain Input Shaping for Closed-Loop Discrete-Time Systems

Uwe Boettcher, Raymond A. de Callafon and Frank E. Talke*

* *University of California, San Diego, Center for Magnetic Recording Research , 9500 Gilman Drive, M/C 0401, La Jolla , CA 92093 USA (e-mail: uwe@ucsd.edu)*

Abstract: An input shaping algorithm based on convex optimization techniques is presented for closed-loop discrete-time linear time-invariant (LTI) systems where closed-loop signals are subject to linear constraints. As an illustrative example the seeking process in a Hard Disk Drive is investigated. The closed-loop system responses to both shaped and non-shaped inputs are compared.

1. INTRODUCTION

For linear time-invariant (LTI) systems that are subject to a change from an initial state to a target state, input shaping is a powerful technique to reduce residual vibrations in those systems as shown by Singer and Seering (1990). The targeting trajectory can be further optimized (e.g. minimize targeting time or energy consumption) through convex optimization techniques. Those techniques have been widely applied to these problems since they guaranty the convergence to a global optimum. In addition, the recent increase in computational power in control systems justifies their increasing complexity. A broad overview of real-time or nearly real-time applications has been given by Mattingley and Boyd (2010).

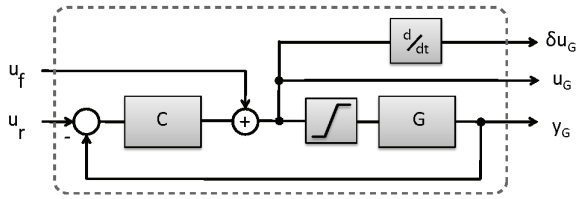

Fig. 1. Closed loop LTI system

Input shaping is usually formulated as an open-loop problem where linear constraints on input and output signals are imposed to formulate a convex optimization problem to find optimal and possible minimal time input profiles. Commonly, finite impulse response (FIR) filters are used to pre-filter input signals as e.g. shown by Pao (1999) for MIMO systems in continuous time and for discrete time systems by Baumgart and Pao (2007).

Some closed-loop approaches are given by Kapila et al. (2000) where input shaping based on FIR filters is also applied to closed-loop systems. Another approach to closed-loop input shaping is the shaped time-optimal servomechanism (STOS) that has been developed by Pao and Laorpacharapan (2004) for continuous time systems. Here, mode switching control turns off the feedback during the targeting stage. Kogiso and Hirata (2009) show the reference signal generation for constrained closed-loop systems based on piecewise affine functions of state and reference vector. In (Sugie and Yamamoto (2001)) and (Suzuki and Sugie (2008)), the reference signal generation is shown for a closed-loop system although time-minimal control is not addressed.

Limited results are available on performing input shaping on closed-loop systems where reference and feedforward signals are computed in the presence of constraints on control and output signals. The computation of optimal reference profiles in closed-loop systems has direct application in high performance servo systems where short-time tracking of set-point values is required.

In this paper, we show an input shaping technique for closed-loop multi-input multi-output (MIMO) LTI systems that use full degree-of-freedom control such as the one shown in Fig. 1. The developed algorithm computes the optimal reference signals u_r and u_f given linear constraints on the output signal y_G, the plant control signal u_G and the reference signals u_r and u_f.

2. DEFINING THE SYSTEM

2.1 Specifications of closed-loop signals

We consider an LTI model of the plant G in Fig. 1 with p inputs and m outputs of order n_G and an LTI model of the controller C with p outputs and m inputs of order n_C. The state space model of G is given by

$$\begin{aligned} x_G(k+1) &= A_G x_G(k) + B_G(u_f(k) + y_C(k)) \\ y_G(k) &= C_G x_G(k) + D_G(u_f(k) + y_C(k)) \end{aligned} \tag{1}$$

and the feedback connection is given by

$$\begin{aligned} x_C(k+1) &= A_C x_C(k) + B_C(u_r(k) - y_G(k)) \\ y_C(k) &= C_C x_C(k) + D_C(u_r(k) - y_G(k)) \end{aligned} \tag{2}$$

In order to specify constraints to the plant input, u_G and the rate of change δu_G must be available as outputs of the closed-loop state-space system as indicated in Fig. 1. Therefore, we add p states to the closed-loop model and define a measurement state vector x_M

$$x_M(k+1) = u_G(k) = y_C(k) + u_f(k) \tag{3}$$

and

$$u_G(k-1) = x_M(k) \tag{4}$$

We can now define the two additional outputs of our closed-loop system

$$\begin{aligned} u_G(k) &= y_C(k) + u_f(k) \\ \delta u_G(k) &= u_G(k) - u_G(k-1) \end{aligned} \tag{5}$$

Furthermore, we define the input vector $u(k) \in \mathbb{R}^{(m+p)\times 1}$, the output vector $y(k) \in \mathbb{R}^{(m+2p)\times 1}$ and the state space vector $x(k) \in \mathbb{R}^{(n_C+n_G+p)\times 1}$ as

$$u(k) = \begin{pmatrix} u_r \\ u_f \end{pmatrix},\ y(k) = \begin{pmatrix} y_G \\ u_G \\ \delta u_G \end{pmatrix},\ x(k) = \begin{pmatrix} x_C \\ x_G \\ x_M \end{pmatrix} \tag{6}$$

Here, $u_r(k)$ and $u_f(k)$ are the computed reference signals.

Using (1)-(6) we can define the state space system of the closed loop system as

$$\begin{aligned} x(k+1) &= Ax(k) + Bu(k) \\ y(k) &= Cx(k) + Du(k) \end{aligned} \tag{7}$$

where the state space matrices are calculated by

$$A = \begin{bmatrix} A_C - B_C M D_G C_C & -B_C M C_G & 0 \\ B_G C_C - B_G D_C M D_G C_C & A_G - B_G D_C M C_G & 0 \\ C_C - D_C M D_G C_C & -D_C M C_G & 0 \end{bmatrix}$$

$$B = \begin{bmatrix} B_C - B_C M D_G D_C & -B_C M D_G \\ B_G D_C - B_G D_C M D_G D_C & B_G - B_G D_C M D_G \\ D_C - D_C M D_G D_C & -D_C M D_G + I \end{bmatrix} \tag{8}$$

$$C = \begin{bmatrix} M D_G C_C & M C_G & 0 \\ C_C - D_C M D_G C_C & -D_C M C_G & 0 \\ C_C - D_C M D_G C_C & -D_C M C_G & -I \end{bmatrix}$$

$$D = \begin{bmatrix} M D_G D_C & M D_G \\ D_C - D_C M D_G D_C & I - D_C M D_G \\ D_C - D_C M D_G D_C & I - D_C M D_G \end{bmatrix}$$

In (8), M is defined as

$$M = (I + D_G D_C)^{-1} \tag{9}$$

The inverse in (9) can be calculated for a well-defined closed-loop system with $D_G D_C \neq -I$. In practical applications most plants will have at least one sample time delay with $D_G = 0$ making $M = I$.

2.2 Explicit solution of the closed-loop system

The output y combines the plant output y_G, the plant input u_G and its rate of change δu_G on which constraints will be imposed. For writing the linear constraints we use (7) and follow Goodwin et al. (2005) (but including the feed-through term D) to write the output equations recursively as

$$\begin{aligned} y(0) &= Cx(0) + Du(0) \\ y(1) &= CAx(0) + CBu(0) + Du(1) \\ y(2) &= CA^2x(0) + CABu(0) + CBu(1) + Du(2) \\ &\vdots \\ y(M) &= CA^M x(0) + \sum_{i=1}^{M} CA^{M-i}Bu(i-1) \\ &\quad + Du_s \\ y(M+1) &= CA^{M+1}x(0) + \sum_{i=1}^{M} CA^{M+1-i}Bu(i-1) \\ &\quad + Du_s + CBu_s \\ &\vdots \\ y(N-1) &= CA^{N-1}x(0) + \sum_{i=1}^{M} CA^{N-i-1}Bu(i-1) + \\ &\quad + Du_s + \sum_{i=1}^{N-M-1} CA^{i-1}Bu_s \end{aligned} \tag{10}$$

where M is the control horizon and N is the optimization horizon. Here, u_s defines the residual reference signal after the control horizon which needs to be set to a constant value. An obvious choice is $u_r = y_{\text{target}}$ and $u_f = 0$ for $k \geq M$. We can now rewrite (10) conveniently in matrix notation by defining $\mathbf{\Psi}$ as

$$\mathbf{\Psi} = \begin{bmatrix} D & 0 & 0 & \cdots & 0 \\ CB & D & 0 & \cdots & 0 \\ CAB & CB & D & \cdots & 0 \\ \vdots & \vdots & \vdots & \ddots & \vdots \\ CA^{M-2}B & CA^{M-3}B & & \cdots & D \\ CA^{M-1}B & CA^{M-2}B & & \cdots & CB \\ CA^{M}B & CA^{M-1}B & & \cdots & CAB \\ \vdots & \vdots & & \ddots & \vdots \\ CA^{N-2}B & CA^{N-3}B & & \cdots & CA^{N-M-1}B \end{bmatrix} \tag{11}$$

Furthermore, we define $\mathbf{\Omega}$, $\mathbf{y}$ and $\mathbf{\Delta}$ as

$$\mathbf{\Omega} = \begin{bmatrix} C \\ CA \\ CA^2 \\ \vdots \\ CA^{N-1} \end{bmatrix}, \mathbf{y} = \begin{bmatrix} y(0) \\ y(1) \\ y(2) \\ \vdots \\ y(N-1) \end{bmatrix}$$

$$\mathbf{\Delta} = \begin{bmatrix} 0 \\ \vdots \\ 0 \\ Du_s \\ Du_s + CBu_s \\ \vdots \\ Du_s + \sum_{i=1}^{N-M-1} CA^{i-1}Bu_s \end{bmatrix} \tag{12}$$

Now, we can rewrite (10) as

$$\mathbf{y} = \mathbf{\Psi u} + \underbrace{\mathbf{\Omega} x(0) + \mathbf{\Delta}}_{\mathbf{q}} \tag{13}$$

where the vector $\mathbf{u}$ contains the input signals

$$\mathbf{u} = [\, u(0), \cdots, u(M-1) \,]^T \tag{14}$$

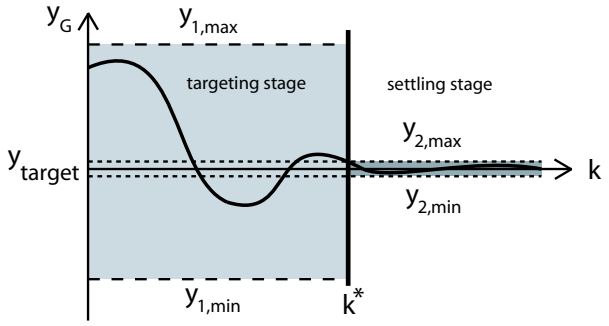

Fig. 2. Definition of the output constraints

and the vector $\mathbf{y}$ contains the output signals for each time step k. Each element itself will be a vector of size $(m+p)\times 1$, respectively. In (13) the explicit input-output relation is linear in $\mathbf{u}$. We shall now proceed to specify the constraints and the optimization routine for input shaping.

3. CONVEX OPTIMIZATION

For a comprehensive overview of convex optimization techniques the reader is referred to Boyd and Vandenberghe (2004). In this paper a specific solution to the closed-loop problem will be given for constraining the signals in (6).

3.1 Constraints on the closed-loop signals

As indicated in Fig. 1, the output y captures all of the relevant closed-loop signals. It contains not only the output of the plant y_G but also the plant input u_G and its rate of change δu_G. In defining constraints on closed-loop signals we refer to the constraints on the output $y = (y_G, u_G, \delta u_G)^T$ in which we distinguish between different signals. The plant output y_G is subject to two different amplitude constraints as indicated in Fig. 2. One constraint is a large amplitude constraint during the targeting stage. We define this constraint by $y_{1,\max}$ and $y_{1,\min}$, respectively. Once the target is reached, a tolerance ϵ of the output from the desired target is specified by

$$y_{2,\min} = y_{\text{target}} - \epsilon \le y \le y_{2,\max} = y_{\text{target}} + \epsilon \qquad (15)$$

creating a tight amplitude constraint during the settling stage. In Fig. 2, k^* denotes the number of samples to reach the target. For all sample numbers $k < k^*$ the targeting output constraints apply, while for all sample numbers $k \ge k^*$ the settling stage (and finally steady state) output constraints apply. Choosing a minimal value for k^* would amount to finding a minimal time solution. We will later use a line search over k^* to find the minimal time solution. For now, k^* is assumed to be given.

Furthermore, we specify constraints on the plant input u_G. We consider amplitude constraints on the input. In addition, the maximum rate of change of the input signal is limited which is commonly introduced through rate limitations in digital-to-analog conversion. In summary, we define amplitude and rate constraints as

$$u_G \le u_{G,max} \quad \delta u_G \le \delta u_{G,max} \qquad (16)$$

and similarly

$$\begin{aligned} u_G \ge u_{G,min} \Leftrightarrow -u_G \le -u_{G,min} \\ -\delta u_G \le -\delta u_{G,min} \end{aligned} \qquad (17)$$

In matrix notation the output constraints can be written as

$$\mathbf{y_{min}}(k^*) \le \mathbf{\Psi u} + \mathbf{q} \le \mathbf{y_{max}}(k^*) \qquad (18)$$

where $\mathbf{y_{max}}$ and $\mathbf{y_{min}}$ are defined by

$$\mathbf{y_{max}}(k^*) = \begin{bmatrix} y_{1,max} \\ u_{G,max} \\ \delta u_{G,max} \\ \vdots \\ y_{2,max} \\ u_{G,max} \\ \delta u_{G,max} \end{bmatrix}, \ \mathbf{y_{min}}(k^*) = \begin{bmatrix} y_{1,min} \\ u_{G,min} \\ \delta u_{G,min} \\ \vdots \\ y_{2,min} \\ u_{G,min} \\ \delta u_{G,min} \end{bmatrix} \qquad (19)$$

3.2 Constraints on reference signals

The reference signals u_r and u_f in Fig. 1 are captured in the input signal u in (7) and (14). By imposing constraints on $\mathbf{u}$ we are now referring to the constraints on the reference inputs u_r and u_f. The reference signals are limited by an amplitude constraint

$$\mathbf{u_{min}} \le \mathbf{u} \le \mathbf{u_{max}} \qquad (20)$$

whereas a rate constraint

$$\delta\mathbf{u_{min}} \le \delta\mathbf{u} \le \delta\mathbf{u_{max}} \qquad (21)$$

can also be included in our approach, where

$$\mathbf{u_{max}} = [\, u_{max}, \cdots, u_{max} \,]^T \qquad (22)$$

$$\delta\mathbf{u_{max}} = [\, \delta u_{max}, \cdots, \delta u_{max} \,]^T \qquad (23)$$

We note that $\mathbf{u_{min}}$ and $\delta\mathbf{u_{min}}$ are defined similarly.

A reference change is defined by

$$\delta u(k) = u(k) - u(k-1) \qquad (24)$$

for each $k \in [0, \cdots, M-1]$. In matrix notation we calculate $\delta\mathbf{u}$ by

$$\delta\mathbf{u} = \mathbf{E}\mathbf{u} \qquad (25)$$

where $\mathbf{E}$ is given by

$$\mathbf{E} = \begin{bmatrix} I_{m+p} & 0 & \cdots & 0 \\ -I_{m+p} & I_{m+p} & \cdots & 0 \\ & \ddots & \ddots & \\ 0 & \cdots & -I_{m+p} & I_{m+p} \end{bmatrix} \qquad (26)$$

and I_{m+p} represents a $(m+p)\times(m+p)$ identity matrix.

3.3 Combined Constraint in Linear Form

All the constraints in (18), (20), (21) and (25) can be combined in one single linear matrix inequality (LMI):

$$\begin{bmatrix} \mathbf{I} \\ -\mathbf{I} \\ \mathbf{E} \\ -\mathbf{E} \\ \mathbf{\Psi} \\ -\mathbf{\Psi} \end{bmatrix} \begin{bmatrix} u(0) \\ \vdots \\ u(M-1) \end{bmatrix} \le \begin{bmatrix} \mathbf{u_{max}} \\ -\mathbf{u_{min}} \\ \delta\mathbf{u_{max}} \\ -\delta\mathbf{u_{min}} \\ \mathbf{y_{max}}(k^*) \\ -\mathbf{y_{min}}(k^*) \end{bmatrix} - \begin{bmatrix} 0 \\ 0 \\ 0 \\ 0 \\ \mathbf{q} \\ -\mathbf{q} \end{bmatrix} \qquad (27)$$

or short

$$\mathbf{L}\mathbf{u} \le \mathbf{W}(\mathbf{k}^*) - \mathbf{Q} \qquad (28)$$

In (27), $\mathbf{I}$ is an $(m+p)M \times (m+p)M$ identity matrix, and $\mathbf{\Psi}$ is given in (11). In (27) and (28) the term $\mathbf{Q}$

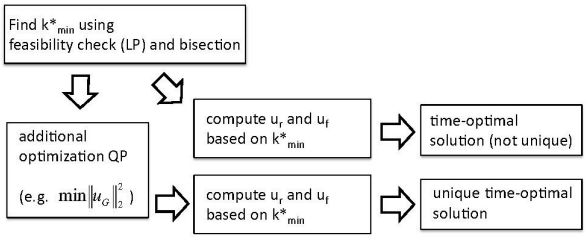

Fig. 3. Optimization algorithm

with $\mathbf{q} = \mathbf{\Omega x(0)} + \mathbf{\Delta}$ represents the effect of initial and residual conditions. It should be noted that $\mathbf{W}$ depends on the choice of k^* in Fig. 2. The additional freedom in k^* will be used to check for a feasible solution of the input shaping problem and to formulate a minimal time solution for settling.

3.4 Feasibility check for time-optimal solution

We can check whether or not the constraints are feasible for a given k^* by solving the following linear program (LP) (Nocedal and Wright (1999); Stamnes and de Callafon (2007)):

$$\begin{aligned} & \min_{u,\,z} \ \mathbf{1}^T\mathbf{z} \\ \text{subject to} \quad & \mathbf{Lu} - \mathbf{z} \le \mathbf{W(k^*)} - \mathbf{Q} \\ & \mathbf{z} \ge 0 \end{aligned} \tag{29}$$

If $\mathbf{z} = 0$ is the optimal solution then the inequality (28) is feasible, otherwise infeasible. In (29) $\mathbf{1} = [1, \cdots, 1]^T$ is a column vector of ones.

In order to obtain the time-optimal solution we solve the LP in (29) several times for different values of k^*. We use a bisection method (Boyd and Vandenberghe (2004)) that results in quadratic convergence to find the minimum sample number k^*_{min} (where $1 \le k^*_{min} \le M$) for a feasible set of constraints. This represents a time-optimal solution to the problem which is not unique. Further optimization in the form of quadratic programming (QP) as indicated in Fig. 3 and described in the next subsection is needed to obtain a unique solution.

3.5 Quadratic programming

The time-optimal (or better time-minimal) trajectory is not always desired. Depending on the application, other parameters might be more important such as e.g. energy consumption. To further improve the energy properties of the signals in the input shaping problem one can pose a quadratic criterion involving both $\mathbf{y}$ and $\mathbf{u}$ given the constraints in (27) and (28). Knowing that a particular value for k^* is able to give a feasible solution from the LP problem in (29), a further refinement of this solution can be found by solving the Quadratic Programming (QP) problem

$$\begin{aligned} & \min_{u,\,y'} \ \mathbf{y'}^T\mathbf{P_1}\mathbf{y'} + \mathbf{u}^T\mathbf{P_2}\mathbf{u} \\ \text{subject to} \quad & \mathbf{Lu} \le \mathbf{W(k^*)} - \mathbf{Q} \\ & \mathbf{y'} = \mathbf{S}\left(\mathbf{\Psi u} + \mathbf{q}\right) \end{aligned} \tag{30}$$

where $\mathbf{P_1}$ and $\mathbf{P_2}$ are semi-positive definite matrices with dimensions of $\mathbf{y'}$ and $\mathbf{u}$, respectively. With $\mathbf{P_1} \ge 0$ and $\mathbf{P_2} \ge 0$, the QP problem is convex. The QP in (30) consists of a quadratic cost function, an inequality constraint linear in $\mathbf{u}$ and and equality constraint linear in $\mathbf{u}$ and $\mathbf{y'}$.

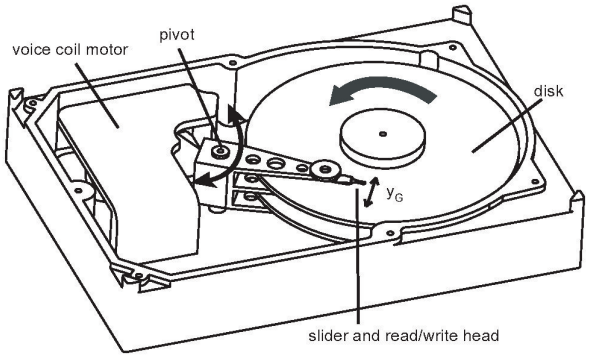

Fig. 4. Main components of a hard disk drive

The introduction of the additional variable $\mathbf{y'}$ and the equality constraint is necessary in order to define constraints on u_G. This increases the complexity of the problem. To keep the variable size of $\mathbf{y'}$ at a minimum, we reduce the original size of $\mathbf{y} \in \mathbb{R}^{(m+2p)\times 1}$ to $\mathbf{y'} \in \mathbb{R}^{p\times 1}$ under the assumption that we want to minimize u_G. This is done by multiplying the equality constraint in (30) by the selection matrix $\mathbf{S}$.

For our particular arrangement defined in (6), we can define the elements of $\mathbf{S}$ as

$$s_{\mathrm{r,c}} = \begin{cases} 1 \text{ for } \mathrm{r} = kp + i, \ \ \mathrm{c} = k(m+2p) + m + i \\ \qquad k \in [0, \cdots, N-1], \ \ i \in [1, \cdots, p] \\ 0 \qquad \text{elsewhere} \end{cases} \tag{31}$$

where r and c are referred as row and column index of $\mathbf{S}$, respectively. The QP in (30) represents only one possible optimization objective, although a very relevant one but there are many other possible objectives. We will now show the effectiveness of the proposed optimization routine by means of an illustrative example.

4. SIMULATION EXAMPLE

4.1 Problem description

We consider the seeking process in a Hard Disk Drive (HDD) as an example. Figure 4 shows the main components of a HDD. The data are stored in circumferential tracks on the disk and the slider with the read/write element is positioned in the radial direction (y_G) to read/write from different tracks. This process is referred as "seeking". The servo actuator in a HDD is a voice coil motor (VCM) that incorporates a double integrator behavior with a low frequency spring (due to pivot-friction) and a set of high frequency resonance modes. For simplification we only assume one main resonance mode at 2 kHz and a well damped low frequency resonance mode at 1 Hz. The transfer function of the actuator is given in continuous time by

$$G = \prod_{i=1}^{2} \frac{K_i\omega_i^2}{s^2 + 2\delta_i\omega_i s + \omega_i^2} \tag{32}$$

with $K_1 = 1$, $K_2 = 10^4$, $\omega_1 = 2\pi 1\frac{1}{\mathrm{s}}$, $\omega_2 = 2\pi 2000\frac{1}{\mathrm{s}}$, $\delta_1 = 1$, $\delta_2 = 0.01$. The system is converted to discrete time

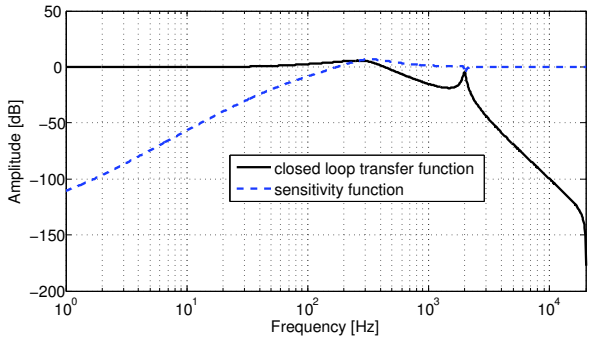

Fig. 5. Amplitude plot of closed-loop transfer function and sensitivity function for both controllers

using zero order hold (ZOH) with a sampling frequency of 40 kHz.

A simple PID controller with high frequency roll-off was designed in discrete-time. The amplitude plots of closed-loop transfer function from reference input to output and the sensitivity function (error rejection function) are shown in Fig. 5. The discrete-time controller is given by

$$C = \frac{3.3496(z-0.9925)^2}{(z-1)(z-0.9252)(z-0.7623)} \tag{33}$$

In this simulation example the feed through-terms of both the controller and the plant are zero, and we consider zero initial conditions ($x(0) = 0$). Three interesting situations that will be explained in the following subsections are investigated:

(1) Small step on desired actuator position
(2) Large step on desired actuator position and "relatively loose bounds" on y_G
(3) Large step on desired actuator position and "relatively tight bounds" on y_G

In all three cases we only assume constraints on u_G and δu_G in addition to the constraints on y_G. We solve the QP according to (30) with $\mathbf{P_1}$ and $\mathbf{P_2}$ being the identity matrix, respectively. When only using feedback and a step-wise change of u_r, the small step on the desired actuator position does not use the full range available within actuator saturation that can be exploited by input shaping. The large steps on the desired actuator position will saturate the actuator input. Input shaping can alleviate this problem. The values of the constraints are: $u_{G,max} = 10\,\text{V}$, $\delta u_{G,max} = 5\,\text{V}$, $y_{1,max} = 2y_{\text{target}}$ and $u_{G,min} = -u_{G,max}$, $\delta u_{G,min} = -\delta u_{G,max}$, $y_{1,min} = -y_{1,max}$. All other values are specific to the particular case and summarized in Tab. 1.

4.2 Case 1: Small step (no actuator saturation)

We simulated a short-distance seek of 1 track using our designed controller C. The constraints were set to be within 10% of the track-pitch which is usually the allowed margin in order to avoid read/write errors. The results are shown in Fig. 6 (gray dashed line). The response is relatively slow and has a considerably high overshoot. This is expected after looking at Fig. 5 that suggests that the closed-loop bandwidth is arround 300 Hz. The plant input

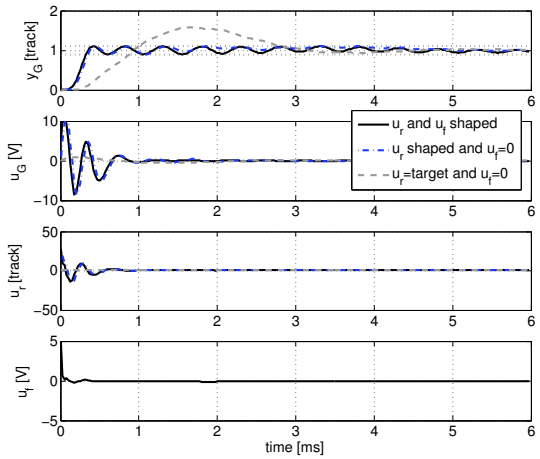

Fig. 6. Case 1: Small step on desired actuator position

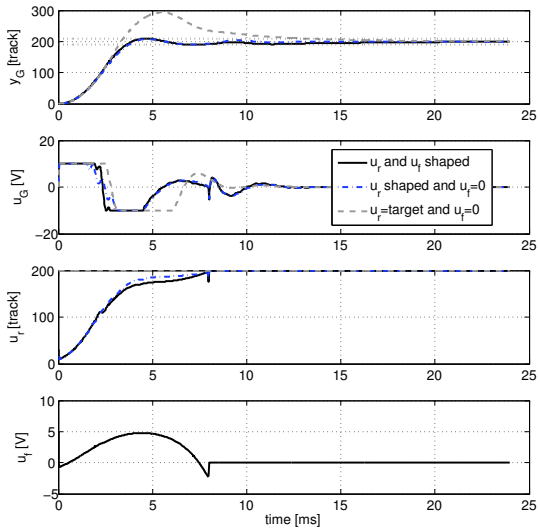

Fig. 7. Case 2: Large step on desired actuator position with actuator saturation

signal u_G is well below the constraint of 10 V. Using the input shaping technique described in sections 2 and 3 we compute the time-minimal input signal with minimized control effort given the constraints defined in *4.1* and Tab. 1. The dash-dotted line in Fig. 6 denotes the case where only u_r is used and the solid line shows the case where full degree-of-freedom (DOF) control is applied (u_r and u_f). Below, we will refer to those three situations as the 0 DOF, 1 DOF and 2 DOF case, respectively. The difference between 1 DOF and 2 DOF is not very large (1 sample); however, they are both much faster than the 0 DOF case as they use u_G to full capacity. The vibrations (within the specified constraints) observed in the output signal correspond to the 2nd resonance mode at 2 kHz and could be lowerd by tightening the constraints on u_G at the expense of a potentially longer seek time.

4.3 Case 2: Large step (actuator saturation)

We now look at a larger step of 200 tracks (Fig. 7) which in general leads to the saturation of u_G. The 0 DOF case (no

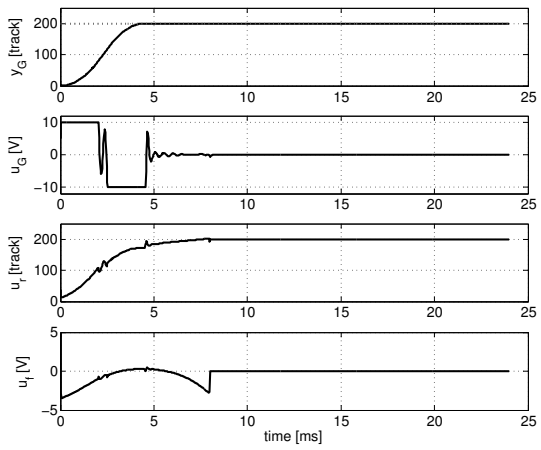

Fig. 8. Case 3: Large step on desired actuator position with tight bounds on y_G

input shaping) has a considerably larger seek time than the 1 DOF and 2 DOF case. The difference in terms of speed between 1 DOF and 2 DOF is slightly larger (5 samples) than in the previous case but is still comparably small. We note that in this simulation ϵ was adjusted according to the increase in y_{target}. Intuitively, this is expected for many positioning systems: The operating range determines the positioning precision. Unfortunately, this is not the case for HDDs as the positioning accuracy needs to be within the same bounds regardless of the size of the step. Thus, ϵ is set back to its nominal value of 0.1.

4.4 Case 3: Large step (actuator saturation) revisited

In Fig. 8 we see the simulation results for case 3 which is the same as case 2 except for a decrease of ϵ by two orders of magnitude. The figure shows only the 2 DOF case where the target was reached after 173 samples. Using only u_r, there was no feasible solution found for any $k^* \leq M$. The computed signal u_G incorporates mainly "bang-bang" control which has been proven to be the time-optimal solution for a perfect double integrator.

Table 1. Simulation parameters

	case 1	case 2	case 3
y_{target}	1	200	200
M	80	320	320
N	240	960	960
ϵ	0.1	10	0.1
k^*_{min} (1 DOF)/(2 DOF)	14/13	150/145	173/($> M$)

5. CONCLUSIONS

An input shaping algorithm for closed-loop discrete-time LTI systems has been described in this paper. It was shown that input shaping significantly reduces targeting time and residual vibrations compared to outputs responses obtained by standard reference signals such as steps. It was also shown that input shaping improves the response of systems whether or not plant saturation is present. Furthermore, it has been seen that 2 DOF versus 1 DOF reference input signal shaping is only beneficial when the output constraints are chosen to be tight during the settling phase.

To draw more detailed conclusions about a practical implementation, further theoretical and experimental studies are necessary. The system was simulated without considering noise. It is anticipated that by assuming a sufficiently high SNR, the noise could be included by simply adjusting (loosening) the constraints as the feedback controller will remove the steady-state error in most cases. Other points to address would be for instance to include parameter variations of the plant and controller models to ensure robustness of the computed time-optimal input reference profiles. Experimental work to further validate the effectiveness of the proposed method of reference signal input shaping is currently under way.

REFERENCES

Baumgart, M.D. and Pao, L.Y. (2007). Discrete time-optimal command shaping. *AUTOMATICA*, 43(8), 1403–1409.

Boyd, S. and Vandenberghe, L. (2004). *Convex Optimization*. Cambridge University Press, New York.

Goodwin, G., Seron, M., and de Dona, J. (2005). *Constrained Control and Estimation: An Optimization Approach*. Springer Verlag, London.

Kapila, V., Tzes, A., and Yan, Q. (2000). Closed-loop input shaping for flexible structures using time-delay control. *Journal of Dynamic Systems, Measurement, and Control*, 122(3), 454–460.

Kogiso, K. and Hirata, K. (2009). Reference governor for constrained systems with time-varying references. *Robotics and Autonomous Systems*, 57(3), 289 – 295. Selected papers from 2006 IEEE International Conference on Multisensor Fusion and Integration (MFI 2006), 2006 IEEE International Conference on Multisensor Fusion and Integration.

Mattingley, J. and Boyd, S. (2010). Real-time convex optimization in signal processing. *IEEE Signal Process. Mag., Special Issue on Convex Optim. for Signal Process.*

Nocedal, J. and Wright, S.J. (1999). *Numerical Optimization*. Springer-Verlag, New York.

Pao, L.Y. (1999). Multi-input shaping design for vibration reduction. *Automatica*, 35(1), 81 – 89.

Pao, L.Y. and La-orpacharapan, C. (2004). Shaped time-optimal feedback controllers for flexible structures. *Journal of Dynamic Systems, Measurement, and Control*, 126(1), 173–186.

Singer, N.C. and Seering, W.P. (1990). Preshaping command inputs to reduce system vibration. *Journal of Dynamic Systems, Measurement, and Control*, 112(1), 76–82.

Stamnes, O.N. and de Callafon, R.A. (2007). Time-optimal input shaping for discrete-time lti systems with application to seek profiles of a hdd system. *Proc. ASME ISPS Conference, Santa Clara, CA, USA*.

Sugie, T. and Yamamoto, H. (2001). Reference management for closed loop systems with state and control constraints. *Proceedings of the American Control Conference Arlington, VA June 25-27, 2001*.

Suzuki, H. and Sugie, T. (2008). Off-line reference shaping of periodic trajectories for constrained systems with uncertainties. *Automatic Control, IEEE Transactions on*, 53(6), 1531 –1535.